Theor Appl Climatol
DOI 10.1007/s00704-015-1476-0

ORIGINAL PAPER

Analysis of extreme rainfall in the Ebre Observatory (Spain)

Núria Pérez-Zanón[1] · M. Carmen Casas-Castillo[2] · Raúl Rodríguez-Solà[3] · Juan Carlos Peña[4] · Anna Rius[4] · J. Germán Solé[5] · Ángel Redaño[6]

Received: 1 April 2014 / Accepted: 13 April 2015

Abstract The relationship between maximum rainfall rates for time intervals between 5 min and 24 h has been studied from almost a century (1905–2003) of rainfall data registered in the Ebre Observatory (Tarragona, Spain). Intensity–duration–frequency (IDF) curves and their master equation for every return period in the location have been obtained, as well as the probable maximum precipitation (PMP) for all the considered durations. In particular, the value of the 1-day PMP has resulted to be 415 mm, very similar to previous estimations of this variable for the same location. Extreme rainfall events recorded in this period have been analyzed and classified according to their temporal scale. Besides the three main classes of cases corresponding to the main meteorological scales, local, mesoscale, and synoptic, a fourth group constituted by complex events with high-intensity rates for a large range of durations has been identified also, indicating the contribution of different scale meteorological processes acting together in the origin of the rainfall. A weighted intensity index taking into account the maximum rainfall rate in representative durations of every meteorological scale has been calculated for every extreme rainfall event in order to reflect their complexity.

✉ M. Carmen Casas-Castillo
m.carmen.casas@upc.edu

[1] Center for Climate Change (C3), Campus Terres de l'Ebre, Universitat Rovira i Virgili, Avda. Remolins, 13-15, Tortosa, Spain

[2] Departament de Física i Enginyeria Nuclear (FEN), EET, Universitat Politècnica de Catalunya, BarcelonaTech (UPC), Campus de Terrassa, Edifici TR2, C/ Colom, 1, 08222 Terrassa, Spain

[3] Departament de Física i Enginyeria Nuclear (FEN), EPSEVG, Universitat Politècnica de Catalunya BarcelonaTech (UPC), Víctor Balaguer s/n, 08800 Vilanova i la Geltrú, Spain

[4] Servei Meteorològic de Catalunya, Berlin, 38-46, 08029 Barcelona, Spain

[5] Observatori de l'Ebre, CSIC-URL, Horta Alta, 38, 43520 Roquetes, Spain

[6] Departament d'Astronomia i Meteorologia (DAM), Facultat de Física, Universitat de Barcelona (UB), Martí i Franqués, 1, 08028 Barcelona, Spain

1 Introduction

Knowledge about spatial distribution and temporal rainfall intensity is essential in meteorology, hydrology, and civil engineering. Rainfall rate behavior in a location has to be considered for planning hydraulic works, roads, and sewage systems and designing rainwater drainage networks in large infrastructures, and evaluate natural risk due to extreme events occurring in the area. As flood is one of the most important natural hazards in mid-latitude Mediterranean areas (Llasat et al. 2013), the main goal of this work is the study of extremely intense rainfall events able to cause flooding and runoff. The intensity–duration–frequency curves (IDF curves) are an important tool for hydrological planning.

Annual mean precipitation registered in the Ebre Observatory (Tarragona, Spain) is around 530 mm, being more than 650 mm in the city of Barcelona. Both are coastal locations of Catalonia (Spain, Fig. 1), a region with a high spatial rainfall variability ranging from less than 400 mm of annual mean precipitation on the western end of the inner area to more than 1250 mm in the highest mountainous zones of the Catalan Pyrenees, and a high seasonal variability (Martínez et al. 2007). Despite the general concordance between the spatial distribution of the mean annual precipitation and daily magnitudes as the maximum daily rainfall or the daily probable maximum precipitation (PMP), remarkable differences were found (Casas et al. 2007, 2008) as a

Q4

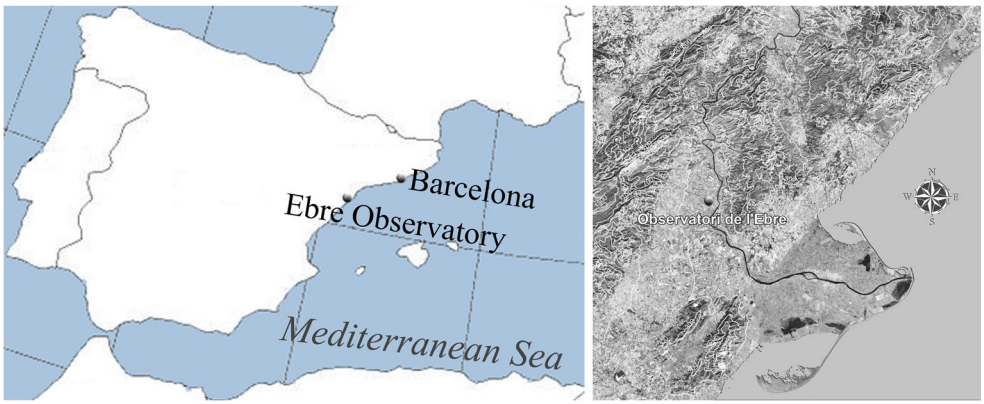

Fig. 1 Geographical situation of the Ebre Observatory. At the *right*, orthophoto of the local area with level curves

consequence of the different meteorological situations contributing to high rainfall amounts for monthly or annual periods (synoptic scale organizations) and those producing the highest rainfall amounts in 1-day time intervals (local and mesoscale systems). There are several studies dedicated to calculate the IDF curves for Barcelona (Lorente and Redaño 1990; Casas et al. 2004; Rodríguez et al. 2014), from the large rainfall data set registered by the Jardí gauge of the Fabra Observatory of the city. In this work, IDF values have been calculated from almost a century of rainfall data (1905–2003) registered in the Ebre Observatory. The relationship between the rainfall intensity values registered for each of the time intervals considered from 5 min to 24 h has been studied for every extreme event recorded in the analyzed period, to investigate the prevailing meteorological temporal scale in each case. The PMP, i.e., "the greatest depth of precipitation for a given duration meteorologically possible for a given size storm area at a particular location at a particular time of year, with no allowance made for long-term climatic trends" (WMO 1986), has been estimated also using a statistical approach.

2 Rainfall rate data statistical analysis

The data set used in this study has been obtained from the digitalization of the strip charts recorded between 1905 and 2003 by two siphon rain gauges located in the Ebre Observatory. These registers were interrupted due to the Spanish civil war for approximately 1 year, from April 4, 1938, to May 1, 1939, so they last 98 years. From these records, the maximum rainfall amounts collected in different time intervals have been obtained. As it is well known, with this type of instrument, it is possible to determine the intensity indirectly from the record of cumulated rainfall to estimate the rainfall amounts in any interval of time. Nevertheless, for short intervals of time as 10 or 20 min, the determination of the intensity can be affected of a not negligible error (between 10 and 15 %). The main cause of this error is, on one hand, the low temporal resolution of the instrument (10 min corresponds approximately to 3 mm of band) and, on the other hand, that the instrument takes between 10 and 20 s to download the accumulated water whenever it gathers the equivalent of 10 mm of rainfall (Lanza et al. 2005). In spite of this, it is not usual to have series of cumulated rainfall so extensive, so complete, and with such verifiable quality like those obtained from this observatory, which can contribute valuable information to the knowledge of the climatology of this variable in this zone. Thus, the maximum rainfall amounts collected in different time intervals between 5 min and 24 h (5, 10, 15, 20, 25, 30, 35, 40, 45, 50, and 55 min, and 1, 2, 6, 12, and 24 h) have been calculated. For each of the 16 considered durations, the two highest values per year have been selected (i.e., a peaks-over-threshold approach considering a return period of 0.5 years as threshold), leading to 16 data series of 196 values each. These series have been considered stationary since no significant trends (p value <0.05) have been detected by a Mann–Kendall test (Yue et al. 2002). In order to analyze their statistical distribution, several theoretic functions have been tested. Among them, the generalized Pareto distribution (GPA) has provided the best fit for the data. The cumulative distribution function of the GPA is defined by Eq. (1),

Q5

$$F(x) = 1 - \left[1 - \kappa\left(\frac{x-\varepsilon}{\alpha}\right)\right]^{\frac{1}{\kappa}} \quad (1)$$

where x is the maximum rainfall amount, ε the location parameter, α the scale parameter, and κ the shape parameter of the GPA distribution. These parameters have been estimated using the L-moments method (Hosking and Wallis 1997). Figure 2 shows the L-moments diagram with the theoretical curve of the GPA distribution fitted to the L-moments values (circles) calculated from the data series. The estimated parameter values for each

Q1

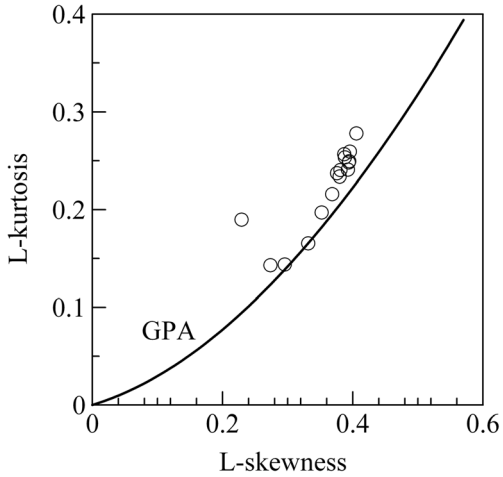

Fig. 2 L-moments diagram calculated for the rainfall data series recorded in the Ebre Observatory (1905–2003). GPA distribution in the *solid line*

of the 16 considered durations are listed in Table 1.

3 Determination of the IDF curves

From the fitted GPA distributions, the estimated maximum rainfall amounts for every duration t and 1-, 2-, 5-, 10-, 25-, 50-, and 100-year return periods T have been determined (Table 2), and so the intensity values $I(t,T)$ shown in Fig. 3. The relationships between these magnitudes are known as IDF curves. Among the different empirical fitting functions used for IDF curves, Sherman's equation (Eq. (2)) (Chen 1983) has been considered to fit the $I(t)$ values for every T,

$$I(t) = \frac{a}{(b+t)^c} \tag{2}$$

where a, b, and c are fitting parameters. Following a method proposed by Chen (1983), these $I(t)$ values have been rescaled using the intensity $I(60,T)$ as rescaling factor to determine a master equation (Casas et al. 2004) relating the three variables $I(t,T)$. The ratio $\frac{I(t,T)}{I(60,T)}$ between the maximum intensity values for each return period and every duration, $I(t,T)$, and the 1-h maximum intensity for the same return period, $I(60,T)$), has been fitted using the Sherman equation (Eq. (2)). The fitting procedure has been done determining first the value of the parameter c which can be related to the temporal scaling properties of the rainfall series (Rodríguez et al. 2014). It has been widely observed that the probability distribution of the annual maximum precipitation intensities satisfies scale relationships (Koutsoyiannis and Foufoula-Georgiu 1993; Burlando and Rosso 1996; Menabde et al. 1999), which means that the probability distribution of the annual maximum intensity for a given duration, i.e., t_0=60 min, $I(60)$, and the distribution at the other scale $I(t)$ (duration $t=\lambda t_0$), will be related by a factor that is a power function of the scale parameter λ, $I(t)=\lambda^{\beta} I(t_0)$, β being a scaling exponent. In terms of the IDF values, the scaling relationship leads to expression (3).

$$I(t,T) = I(60,T)\left(\frac{t}{60}\right)^{\beta} \tag{3}$$

Comparing Eq. (3) and Sherman's equation (Eq. (2)), exponent c can be identified as $-\beta$ if b=0. Casas et al. (2004) and Rodríguez et al. (2014) found a value of b around 10 min for Barcelona, which can be considered small comparing to t for

Table 2 Estimated maximum rainfall amount (in mm) for every duration t and return period T

t (min)	T (years)							
	1	2	5	10	15	25	50	100
5	8.5	10.0	12.0	13.4	14.2	15.3	16.7	18.1
10	12.8	15.6	19.0	21.3	22.6	24.1	26.1	27.8
15	15.9	19.5	23.9	27.1	28.9	31.0	33.8	36.4
20	18.1	22.3	27.7	31.7	34.0	36.8	40.5	44.2
25	19.7	24.5	30.9	35.7	38.4	41.9	46.5	51.1
30	21.0	26.4	33.5	38.9	42.1	46.2	51.7	57.3
35	22.2	28.0	35.9	42.0	45.7	50.3	56.9	63.5
40	23.3	29.5	38.2	45.0	49.1	54.5	62.0	69.8
45	24.3	30.9	40.2	47.6	52.1	58.0	66.2	74.9
50	25.2	32.2	42.0	49.9	54.7	61.0	70.0	79.5
55	26.0	33.2	43.5	51.9	57.0	63.7	73.3	83.6
60	26.7	34.2	44.8	53.5	58.8	65.8	75.8	86.5
120	32.7	42.4	56.5	68.2	75.5	85.2	99.3	114.6
360	42.7	55.2	73.4	88.5	98.0	110.6	129.0	149.1
720	50.6	64.7	85.6	103.3	114.5	129.5	151.8	176.3
1440	58.8	76.5	102.6	124.4	138.1	156.4	183.3	212.6

Table 1 GPA distribution parameters ε (location), α (scale), and κ (shape) estimated using the L-moments method, for each of the 16 considered durations t

t (min)	5	10	15	20	25	30	35	40	45	50	55	60	120	360	720	1440
ε	7.01	9.72	12.09	13.7	14.74	15.75	16.62	17.27	17.92	18.61	19.2	19.67	23.81	31.27	37.8	42.51
α	2.19	4.6	5.62	6.35	7.13	7.59	8	8.49	8.95	9.26	9.51	9.81	12.36	15.84	17.54	22.43
κ	0.018	0.118	0.079	0.038	0.014	−0.013	−0.038	−0.057	−0.067	−0.079	−0.089	−0.091	−0.117	−0.121	−0.142	−0.128

JmlID 704_ArtID 1476_Proof# 1 - 18/04/2015

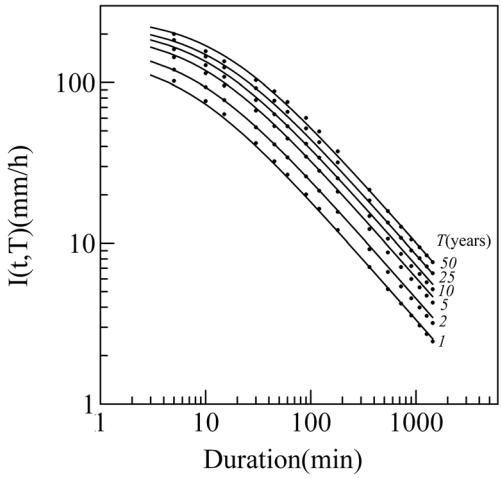

Fig. 3 Intensity values $I(t,T)$ (in mm/h) for durations t between 5 min and 24 h and return periods from 1 to 50 years, and IDF curves

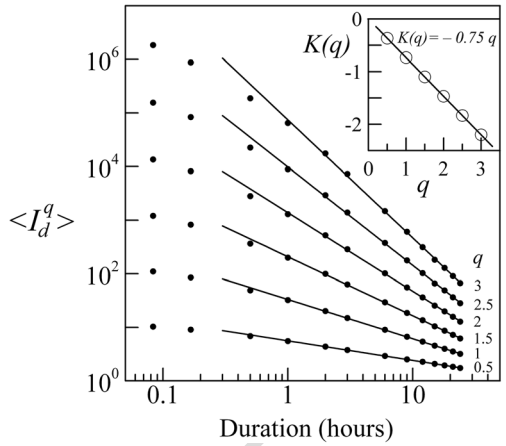

Fig. 4 Statistical moments for different values of q of the annual maximum intensity of the Ebre series, as a function of the duration (between 5 min and 24 h). The *fitted straight lines* indicate scale invariance over the range from 1 to 24 h. Their slopes determine the scale function $K(q)$. The *inserted figure* shows a linear regression between $K(q)$ and the order q of the moments

durations larger than 1 h. This scaling exponent β has been calculated for the annual maximum rainfall series registered in the Ebre Observatory using their statistical moments as proposed by Menabde et al. (1999). The scaling relationship between distributions can be expressed in terms of their moments of order q, $\langle I_d^q \rangle = \lambda^{K(q)} \left\langle I_{d_0}^q \right\rangle$. If the scale function $K(q)$ is linear, $K(q)=\beta q$, the process is a simple scale process or monofractal. If not, the process is multiscalar or multifractal. A simple scaling regime between 1 and 24 h with a value of $\beta=-0.75$ has been found (Fig. 4). Then, the ratio $\frac{I(t,T)}{I(60,T)}$ has then been fitted to Sherman's equation (Eq. (2)) fixing parameter c as 0.75 (±0.1). The obtained parameters a and b have been listed in Table 3. Whereas parameter a resulted very similar for every return period (mean value of 23.9, close to $(1/60)^{-0.75}$, with a standard deviation of 0.5), parameter b is slightly different for every return period (between 6 and 16 min; see Table 3). The behavior of parameter b with return period T can be described by a power expression as $b=6.9T^{0.19}$ (6.9±0.2, 0.19±0.01). Considering this, the fitting by Sherman's equation has been found to be Eq. (4),

$$\frac{I(t,T)}{I(60,T)} = \frac{23.9}{\left(6.9\,T^{0.19}+t\right)^{0.75}} \tag{4}$$

where $I(t, T)$ is the maximum intensity in millimeters per minute for a duration of t minutes with a T-year return period. The intensity of reference $I(60,T)$ shows in turn a logarithmic dependence with the return period T (Eq. 5),

$$I(60,T) = 0.496 \log T + 0.42 \tag{5}$$

where T is expressed in years and the intensity $I(60,T)$ in millimeters per minute. Combining Eqs. (4) and (5), the master equation for the IDF curves of the Ebre Observatory has been obtained (Eq. 6).

$$I(t,T) = \frac{11.9 \log T + 9.9}{\left(6.9\,T^{0.19}+t\right)^{0.75}} \tag{6}$$

The parameters of the numerator in Eq. (6) have been found to be 11.9±0.6 and 9.9±0.6.

This master equation fits satisfactorily the IDF points of Table 2 with a relative error lower than 5 % for durations between 5 min and 6 h and return periods from 1 to 50 years. For the remaining cases, the error is lower than 10 %, as expected considering the uncertainties found for every parameter of Eq. (6). The corresponding curves to the 1-, 2-, 5-, 10-, 25-, and 50-year return periods have been shown in Fig. 3.

4 Classification of extreme rainfall events

From the Ebre Observatory records, rainfall events showing intensities equal to or larger than the 10-year return period intensity values given by Eq. (6) for any duration have been selected. The considered durations have been the 16 time

Table 3 Fitting parameters a and b for every return period T

T (years)	a	b
1	23.1	6.6
2	23.5	7.9
5	23.7	9.7
10	23.9	10.7
15	23.9	11.8
25	24.1	12.8
50	23.9	13.9
100	24.7	16.1

intervals listed in Tables 2 and 5 more (180, 540, 900, 1080, and 1260 min) added to complete the rainfall information between 2 and 24 h in order to obtain a better representation of this temporal period. In the analyzed 98-year period, 28 rainfall events have reached or exceeded these intensities in one or more of the studied durations, 71 % of them occurring in autumn. The relationship between the recorded rainfall amounts for every time interval may provide useful information on the origin and nature of the rainfall. Cluster analysis (Anderberg 1973) is an appropriate technique to investigate this relationship and classify the extreme events based on their similarity (Romero et al. 1999; Casas et al. 2004, 2010). Every rainfall event i is characterized by n measured or calculated variables (x_i^1, x_i^2,…, x_i^n). These variables can be considered as coordinates representing the i rainfall event in an n-dimensional space, so the similarity concept between the events can be specified based on the Euclidean distance between the corresponding points in this n-dimensional space. The process leading to the clusters or groups selection is agglomerative. Among the different clustering procedures, the UPGMA (unweighted pair group method using arithmetic averages), one of the most widely used, has been chosen. The main reason of this choice is that the use of this aggregation method resulted in the better adapted dendrogram to our aim of relating the obtained clusters to the temporal scales of the meteorological processes that originate the storms. The UPGMA usually provides clusters neither too big nor small, with similar and small variances, and not too sensitive to the presence of outliers in the sample. Using UPGMA, the distance between two clusters is defined as the averaged distance between every pair formed by an event from one cluster and another from the other one. The variables used to characterize every one of the selected 28 rainfall events are the 21 recorded maximum rainfall rates within the analyzed time intervals. The obtained dendrogram is shown in Fig. 5, where the nearest (so more similar) events are those connected by the shortest path along the branches. The first vertical line drawn (grey line L1) intersecting the hierarchical tree divides one group of events (group IV in Fig. 5) from the rest of the cases. This group is constituted by events 181040, 191065, 260992, and 150943 (ddmmyy format), showing a high rainfall intensity (T>10 years) for a wide range of durations. Three of them exceed the imposed threshold between 10 min and 24 h, and the remaining one does for the whole considered temporal range (5 min–24 h). These rainfall events, which caused rain flood in the area, are the most complex storms and show the joint action of processes corresponding to more than one of the meteorological scales, as well as the events classified in group IV by Casas et al. (2004, 2010) for extreme storms

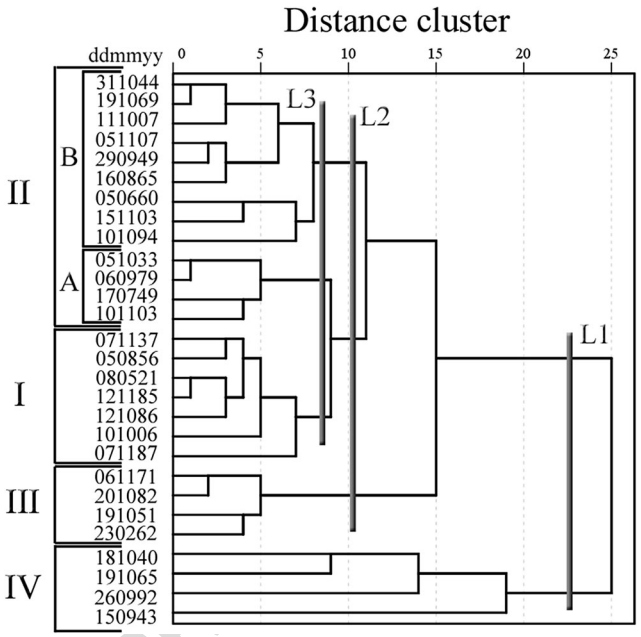

Fig. 5 Dendrogram of the 28 selected extreme rainfall events (*ddmmyy*)

recorded in Barcelona. The synoptic situations corresponding to this kind of complex events (14 % of the studied cases) are characterized by the presence of a depression located SW of the Iberian Peninsula and a powerful blocking anticyclone on the European continent. In some cases (Fig. 6), the depression is clearly reflected on the surface, as happened on event 260992, whereas in others, it only appears in height being much weaker or nonexistent on the surface (Fig. 7). In these situations, the prevailing wind on Catalonia is from the S or SW in medium and high levels, while at 850 hPa and on the surface, the wind has a strong component of E, resulting in a moist and warm advection from the Mediterranean Sea. These situations produce long-lasting advective precipitation (large scale) at the same time that convective phenomena linked to the SE warm flow in low levels, as mesoscale convective systems with even embedded smaller convective cells, cause extreme intense rainfall. Drawing a second vertical line (grey line L2, Fig. 5), three more groups can be identified. Four events (group III in Fig. 5) have a clear synoptic origin. The other two groups are group IIB and a large ensemble that can be divided using a third vertical line (grey line L3) into groups I and IIA. Group I is formed by seven events reaching high rainfall rate values (return period equal to or larger than 10 years) only for durations equal to or shorter than 15 min and lower values for the rest, whereas the four events of group IIA show high rates till 35–60 min. Group I is representative of extremely local or microscale rainfall events, with a clear seasonal influence (seven of the eight cases were recorded between August and

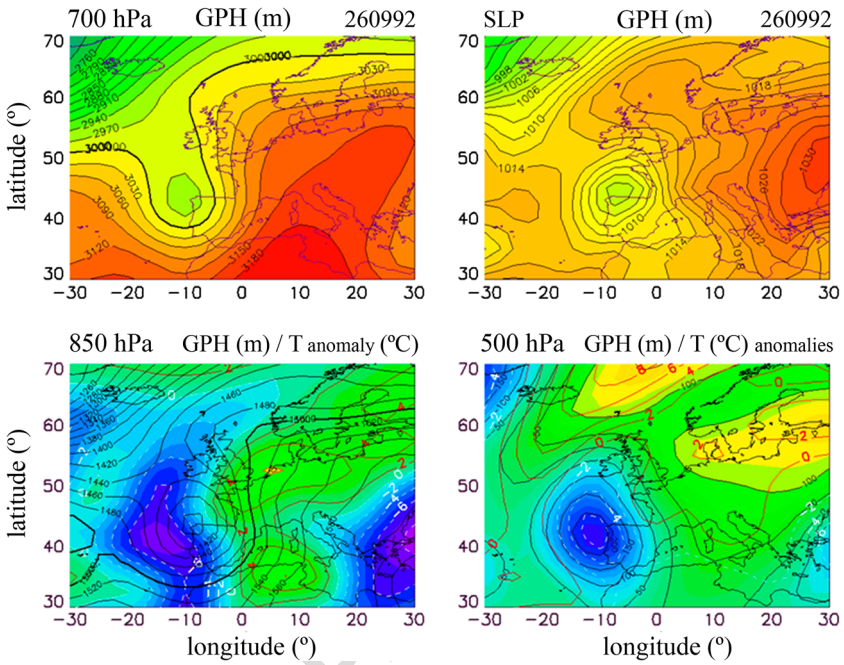

Fig. 6 Synoptic situation corresponding to the event 260992 at the sea surface level (sea level pressure (SLP)) and 850, 700, and 500 hPa. The geopotential height and its anomaly at 500 hPa are measured in meters. The temperature anomaly at 850 and 500 hPa is measured in degrees Celsius. Data obtained from the 20th Century V2 Reanalysis Project (20CRP) provided by NOAA/OAR/ESRL PSD, Boulder, CO (Compo et al. 2011)

Q6

November) and an evident diurnal surface heating effect in the convective development (almost all cases took place after midday). Group IIA can be identified as meso-γ-scale convective systems, at the edge of micro-scale, whereas group IIB events, with high intensities even for 12–24 h, are compatible with meso-α and meso-β scales (Thunis and Bornstein 1996). The meteorological situations causing this type of rainfall in the Mediterranean area are often very active fronts moving slowly with intense mesoscale rainfall systems developed inside (Houze and Hobbs 1982; Browning 1990), or mesoscale convective complexes (Codina et al. 1997).

5 Rainfall intensity weighted index

Casas et al. (2004) proposed a rainfall intensity weighted index (IP) to reflect the severity and complexity of the registered

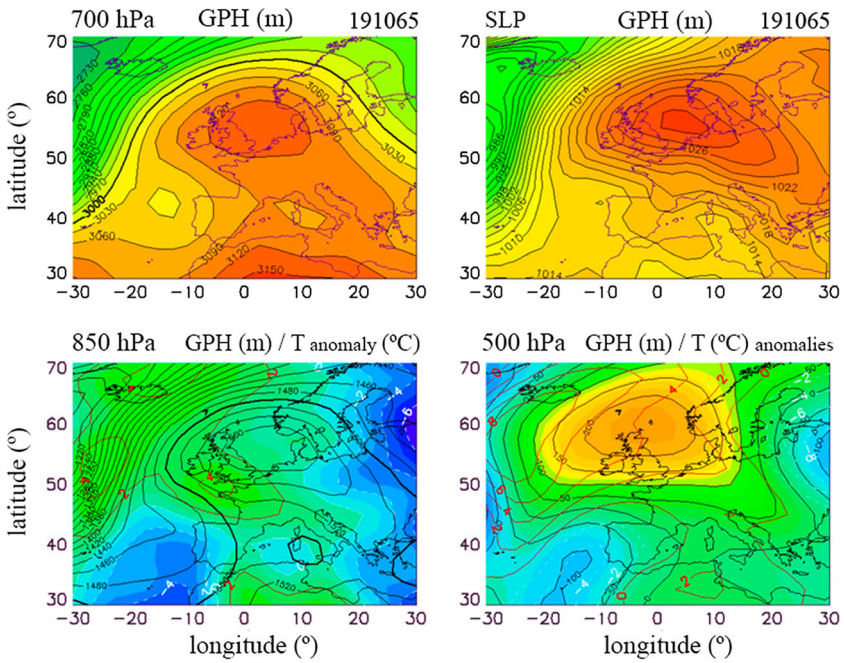

Fig. 7 Synoptic situation corresponding to the event 191065 at the sea surface level (SLP) and 850, 700, and 500 hPa. The geopotential height and its anomaly at 500 hPa are measured in meters. The temperature anomaly at 850 and 500 hPa is measured in degrees Celsius. Data obtained from the 20th Century V2 Reanalysis Project (20CRP) provided by NOAA/OAR/ESRL PSD, Boulder, CO (Compo et al. 2011)

JrnlID 704_ArtID 1476_Proof# 1 - 18/04/2015

Q1

rainfall events according to the contribution of the different meteorological scales to the origin of rainfall (Pinto et al. 2013). For each storm, the maximum intensities I_5, I_{60}, I_{120}, and I_{1440}, corresponding to 5-min and 1-, 2-, and 24-h durations, respectively, are selected as rainfall rate indexes to represent the local scale, small mesoscale, large mesoscale, and synoptic scale contributions. The intensity weighted index IP is defined by Eq. 7,

$$\mathrm{IP}(T) = {}^{1}/_{4}\left\{\frac{I_5}{I(5,T)} + \frac{I_{60}}{I(60,T)} + \frac{I_{120}}{I(120,T)} + \frac{I_{1440}}{I(1440,T)}\right\} \quad (7)$$

where T is the chosen return period for the index normalization. The highest values of the IP are reached usually in storms presenting high rainfall intensities for each of the time intervals corresponding to every meteorological scale, even though a singular storm could have a high IP index for the extraordinary contribution of an only meteorological scale. This index can be useful to provide complementary information to the cluster analysis performed in the former section quantifying the degree of exceptionality of each individual storm. Choosing T as 10 years, the IP for the 28 extreme rainfall events has been calculated (Fig. 8). As expected, the highest indexes correspond to the complex rainfall events classified into group IV, with values higher than 1.26, and two events classified as group IIB by the cluster analysis have an IP value higher than 1. It is remarkable that 68 % of the studied rainfall events only achieved the imposed intensity level in one or none of the selected representative durations, seven of the nine remaining cases show 10-year return period intensities in two or three time intervals, and only two of the events have reached them in the four durations simultaneously.

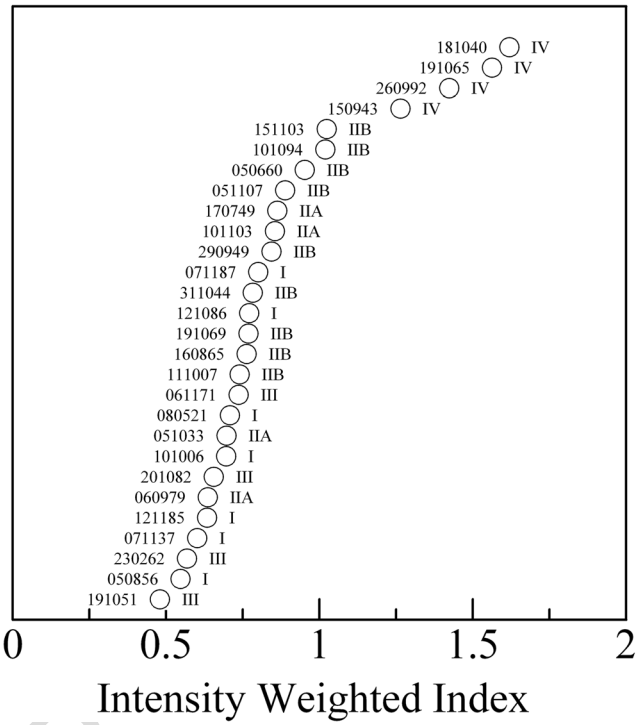

Fig. 8 IP index showing the severity and complexity of the classified extreme rainfall events

6 Maximum probable precipitation estimation

Hydrologists use the PMP magnitude and its spatial and temporal distributions to calculate the probable maximum flood (PMF), which is one of several conceptual flood events used in the design of hydrological structures, for maximum reliability and safety. Procedures for determining the PMP are admittedly inexact: results are estimates and a risk statement has to be assigned to them. Quoting Koutsoyiannis (1999), the PMP approach "by no means implies zero risk in reality." The National Research Council (1994) estimates the return period of the PMP in the USA as between 10^5 and 10^9 years. To estimate the PMP in a place, a variety of procedures based on the location of the project basin, availability of data, and other considerations have been proposed (e.g., Wiesner 1970; Schreiner and Reidel 1978; WMO 1986; Collier and Hardaker 1996). Most of them are based on meteorological analysis, while some are based on statistical analysis. Among the statistical methods for estimating the PMP, the most widely used is the method of Hershfield (1961, 1965), based on the frequency analysis of the annual maximum rainfall data registered at the site of interest. In order to estimate the PMP in the area of study, for durations from 5 min to 24 h, the Hershfield statistical method has been applied to rainfall data from the Ebre Observatory (1905–2003).

Table 4 Mean $\bar{x}_n$, coefficient of variation CV, maximum value x_M, and observed frequency factor k_m of the Ebre Observatory annual maximum rainfall series for durations t from 5 min to 24 h

t (min)	$\bar{x}_n$ (mm)	CV	x_M (mm)	k_m
5	9.2	0.3	19.6	3.5
10	14.2	0.4	30.5	3.3
30	24.5	0.4	68.3	4.8
60	32.3	0.5	98.9	4.7
120	40.4	0.5	138.6	5.2
180	44.8	0.5	166.9	6.0
360	54.0	0.5	176.4	5.0
540	60.0	0.5	218.6	6.3
720	64.8	0.5	228.5	6.1
900	68.1	0.5	235.9	5.9
1080	71.7	0.5	243.5	5.4
1260	74.2	0.5	250.6	5.3
1440	76.4	0.5	257.6	5.2

t5.1 **Table 5** PMP values in the Ebre Observatory for every considered duration t in minutes

t (min)	5	10	30	60	120	180	360	540	720	900	1080	1260	1440
PMP (mm)	36	59	112	168	224	250	290	319	338	354	384	400	416
Error (mm)	3	5	10	15	20	23	26	29	30	32	35	36	38

The Hershfield technique for estimating the PMP is based on Chow's (1951) general frequency Eqs. (8) and (9),

$$\mathrm{PMP} = \bar{x}_n + k_m \sigma_n \tag{8}$$

$$k_m = \frac{x_M - \bar{x}_{n-1}}{\sigma_{n-1}} \tag{9}$$

where x_M, $\bar{x}_n$, and σ_n are the highest, mean, and standard deviation for a series of n annual maximum rainfall values of a given duration, $\bar{x}_{n-1}$ and σ_{n-1} are respectively the mean and standard deviation for this series excluding the highest value x_M, and k_m is a frequency factor. Since the frequency factor is the number of standard deviations σ_{n-1} to be added to the mean $\bar{x}_{n-1}$ to achieve the maximum x_M, its value results higher for series including an extraordinarily extreme rainfall event (or *outlier*). The inclusion of an *outlier*, with a recurrence period much longer than the length of the series, could cause an anomalous effect in the calculated mean and standard deviation values (Hershfield 1961). In a previous work (Casas et al. 2008), the 1-day PMP values at 145 locations in Catalonia were estimated following Hershfield's procedure. From their annual maximum daily rainfall series, different statistical parameters including frequency factors, k_m, were calculated. Based on the 145 stations, the k_m values were plotted against the mean $\bar{x}_n$, in order to consider an appropriate enveloping curve that would give reliable estimates of 1-day PMP for Catalonia (Rakhecha et al. 1992). One of the 145 stations used was the Ebre Observatory, with a 46-year annual maximum daily rainfall series obtained from the records of a totalizer rain gauge between 1939 and 1985. The equation corresponds to the enveloping curve ($k_m = -7.56 \ln \bar{x}_n + 40.5$) assigned a frequency factor of k_m=7.3 to the mean daily rainfall value of 81.0 mm in the Ebre Observatory, resulting in an estimated 1-day PMP of 396 mm for this station.

From the 98-year annual series of true maximum rainfall amounts for durations between 5 min and 24 h recorded by the siphon pluviograph, a new statistical estimation of the PMP in the Ebre Observatory has been done. These are true maxima because amounts were calculated using unrestricted time intervals by any particular observation time, instead of the usual fixed intervals between a beginning and an ending time. Table 4 shows the statistical parameters and the observed frequency factors for every considered duration. The mean value of the annual maximum rainfall in 24 h registered by the siphon gauge in the period 1905–2003 is 76.4 mm (see Table 4). The WMO (1986) recommends a multiplicative factor of 1.13 for annual maximum rainfall amounts registered in a single fixed time interval to yield values closely approximating those obtained from analysis based on true maxima. Thus, considering this adjusting factor, the mean true rainfall amount of 76.4 mm in 24 h would approximately correspond to an amount of 67.6 mm for a 24-h fixed interval. The enveloping curve obtained by Casas et al. (2008) assigns to this mean value a frequency factor of 8.6, higher than any of the observed frequency factors varying from 3.3 and 6.3 (Table 4). The highest frequency factors have been found for durations between 3 and 15 h, presenting a maximum of 6.3 for approximately 9 h. This result seems to be related to the meteorological scale of the most severe rain events registered in our region, which are generally related to some of the following mechanisms: deep convection, very active fronts, orographic uplift, mesoscale convective systems, and, very often, the presence of a low-level cyclonic center (Jansà et al. 2001). All these meteorological organizations, producing precipitation with very high efficiency, are included typically into the β-mesoscale with characteristic durations from 2 and 10 h. As the purpose of our work is to obtain PMP, the maximum value 8.6 has been considered as a maximized frequency factor for any duration. In fact, for the same location, the frequency factor k_m for an established return period should be expected not to depend on the duration (Koutsoyiannis 1999). Using Eq. (8), the PMP for every duration t has been calculated (Table 5, Fig. 9). The uncertainty of the PMP values has been determined using a method proposed by Salas et al. (2014) for statistical estimations of the PMP based on Hershfield's technique. This uncertainty has resulted lower than 10 % for each

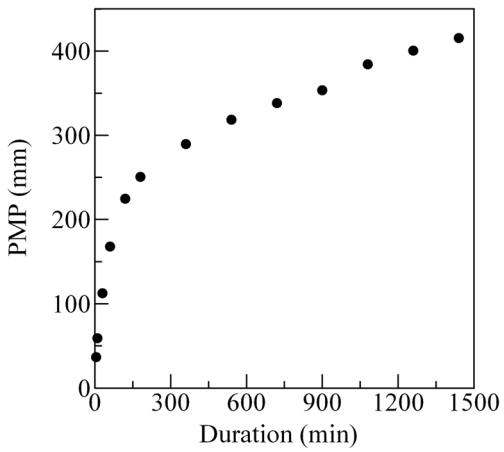

Fig. 9 PMP values for durations between 5 min and 24 h

of the considered durations. The value of the 1-day PMP has been estimated as 416±38 mm, a range in which the value of 396 mm found by Casas et al. (2008) for the same location is included.

7 Conclusions

The maximum rainfall amounts corresponding to time intervals between 5 min and 24 h, obtained from the digitalization of the strip charts recorded by two siphon rain gauges located in the Ebre Observatory between 1905 and 2003, have been satisfactorily fitted to a GPA distribution function. The master equation of the IDF curves in the location $I(t,T) = \frac{11.9\,\log T + 9.9}{\left(6.9\,T^{0.19}+t\right)^{0.75}}$ has been obtained.

Extreme rainfall events recorded in the Ebre Observatory showing a return period equal to or longer than 10 years for any of the considered durations from 5 min to 24 h have been selected. Seventy-one percent of these events occurred in autumn. Using a cluster analysis technique, these events have been characterized and classified into four clearly differentiated groups. The first group contains high-intensity storms with very short durations (equal to or shorter than 15 min), representing the local rainfall events showing a clear seasonal influence and diurnal cycle. The second group corresponds to the typical mesoscale durations, whereas synoptic rainfall events with intensities exceeding the 10-year return period level only for time intervals higher than 9 h constitute the third group. Finally, a rainfall pattern showing high rates for a large range of durations from 10 min to 24 h has been found, associated to local, meso-, and synoptic scale meteorological processes acting together. The synoptic situations corresponding to this kind of complex events (14 % of the studied cases) are characterized by the presence of a depression located SW of the Iberian Peninsula and a powerful blocking anticyclone on the European continent. In these situations, the prevailing wind on Catalonia at 850 hPa and on the surface is from the SE, resulting in a moist and warm advection from the Mediterranean Sea. These situations produce long-lasting advective precipitation at the same time that convective phenomena linked to the SE warm flow in low levels cause extreme intense rainfall. A weighted intensity index taking into account the maximum rainfall rate in the 5-min, 1-h, 2-h, and 24-h time intervals has been calculated for every extreme rainfall event in order to reflect the contribution of every meteorological scale in the origin of rainfall and their complexity.

The PMP in the location for durations between 5 min and 24 h has been estimated using a statistical technique. A value of 415 (±38 mm) has been estimated for the 1-day PMP, very similar to the value of 396 mm found by Casas et al. (2008) for the same location.

Acknowledgments We gratefully acknowledge Eduard Redaño for his contribution in the elaboration of figures. We also acknowledge the Servei Meteorològic de Catalunya (Generalitat de Catalunya) and Observatori de l'Ebre for providing the data analyzed in this work.

References

Anderberg MR (1973) Cluster analysis for applications. Academic, New York, **359 pp**

Browning KA (1990) Organization of clouds and precipitation in extratropical cyclones. Extratropical cyclones. American Meteorological Society, Boston, **262 pp**

Burlando P, Rosso R (1996) Scaling and multiscaling models of depth-duration-frequency curves for storm precipitation. J Hydrol 187:45–64

Casas MC, Codina B, Redaño A, Lorente J (2004) A methodology to classify extreme rainfall events in the western Mediterranean area. Theor Appl Climatol 77:139–150

Casas MC, Herrero M, Ninyerola M, Pons X, Rodríguez R, Rius A, Redaño A (2007) Analysis and objective mapping of extreme daily rainfall in Catalonia. Int J Climatol 27:399–409

Casas MC, Rodríguez R, Nieto R, Redaño A (2008) The estimation of probable maximum precipitation: the case of Catalonia. Trends Dir Clim Res Ann N Y Acad Sci 1146:291–302

Casas MC, Rodríguez R, Redaño A (2010) Analysis of extreme rainfall in Barcelona using a microscale rain gauge network. Meteorol Appl 17:117–123, **http://hdl.handle.net/2117/6733**

Chen C (1983) Rainfall intensity-duration-frequency formulas. J Hydraul Eng 109(12):1603–1621

Chow VT (1951) A general formula for hydrologic frequency analysis. Trans Am Geophys Union 32:231–237

Codina B, Aran M, Young S, Redaño A (1997) Prediction of a mesoscale convective system over Catalonia (northeastern Spain) with a nested numerical model. Meteorol Atmos Phys 62:9–22

Collier CG, Hardaker PJ (1996) Estimating probable maximum precipitation using a storm model approach. J Hydrol 183:277–306

Compo GP, Whitaker JS, Sardeshmukh PD, Matsui N, Allan RJ, Yin X, Gleason BE, Vose RS, Rutledge G, Bessemoulin P, Brönnimann S, Brunet M, Crouthamel RI, Grant AN, Groisman PY, Jones PD, Kruk MC, Kruger AC, Marshall GJ, Maugeri M, Mok HY, Nordli Ø, Ross TF, Trigo RM, Wang XL, Woodruff SD, Worley SJ (2011) The twentieth century reanalysis project. Q J R Meteorol Soc 137(Nordli O):1–28. doi:10.1002/qj.776

Council NR (1994) Estimating bounds on extreme precipitation events. National Academy Press, Washington, DC

Hershfield DM (1961) Estimating the probable maximum precipitation. Proceedings American Society of Civil Engineers. J Hydraul Div 87(HY5):99–106

Hershfield DM (1965) Method for estimating probable maximum precipitation. J Am Waterworks Assoc 57:965–972

Hosking JRM, Wallis JR (1997) Regional frequency analysis: an approach based on L-moments. Cambridge University Press, Cambridge, **224 pp**

Houze RA, Hobbs PV (1982) Organization and structure of precipitating cloud systems. Adv Geophys 24:225–315, **Academic Press**

Jansà A, Genoves A, Picornell MA, Campins J, Riosalido R, Carretero O (2001) Western Mediterranean cyclones and heavy rain. Part 2: statistical approach. Meteorol Appl 8(1):43–56

Koutsoyiannis D (1999) A probabilistic view of Hershfield's method for estimating probable maximum precipitation. Water Resour Res 35(4):1313–1322

Koutsoyiannis D, Foufoula-Georgiu E (1993) A scaling model of storm hyetograph. Water Resour Res 29(7):2345–2361

Lanza LG, Leroy M, Alexadropoulos C, Stagi L,Wauben W (2005) WMO laboratory intercomparison of rainfall intensity gauges—final report. IOM Report No. 84, WMO/TD No. 1304, 2005

Llasat MC, Llasat-Botija M, Petrucci O, Pasqua AA, Rossello J, Vinet F, Boissier L (2013) Towards a database on societal impact of Mediterranean floods within the framework of the HYMEX project. Nat Hazards Earth Syst Sci 13(5):1337–1350. doi:10.5194/nhess-13-1337-2013

Lorente J, Redaño A (1990) Rainfall rate distribution in a local scale: the case of Barcelona City. Theor Appl Climatol 41:23–32

Martínez MD, Lana X, Burgueño A, Serra C (2007) Spatial and temporal daily rainfall regime in Catalonia (NE Spain) derived from four precipitation indices, years 1950–2000. Int J Climatol 27:123–138

Menabde M, Seed A, Pegram G (1999) A simple scaling model for extreme rainfall. Water Resour Res 35(1):335–339

Pinto JG, Ulbrich S, Parodi A, Rudari R, Boni G, Ulbrich U (2013) Identification and ranking of extraordinary rainfall events over northwest Italy: the role of Atlantic moisture. J Geophys Res-Atmos 118(5):2085–2097

Rakhecha PR, Deshpande NR, Soman MK (1992) Probable maximum precipitation for a 2-day duration over the Indian peninsula. Theor Appl Climatol 45:277–283

Rodríguez R, Navarro X, Casas MC, Ribalaygua J, Russo B, Pouget L, Redaño A (2014) Influence of climate change on IDF curves for the metropolitan area of Barcelona (Spain). Int J Climatol 34(3):643–654. doi:10.1002/joc.3712, **http://hdl.handle.net/2117/19960**

Romero R, Ramis C, Guijarro JA (1999) Daily rainfall patterns in the Spanish Mediterranean area: an objective classification. Int J Climatol 19:95–112

Salas JD, Gavilán G, Salas FR, Julien PY, Abdullah J (2014) Uncertainty of the PMP and PMF. Handbook of engineering hydrology: modeling, climate change, and variability, Book II: 575–603. Edited by Saeid Eslamian. CRC Press, Taylor & Francis Group

Schreiner LC, Reidel JT (1978) Probable maximum precipitation estimates. United States east of 105th meridian. Hydrometeorological Report 51, U. S. National Weather Service, Washington DC

Thunis P, Bornstein R (1996) Hierarchy of mesoscale flow assumptions and equations. J Atmos Sci 53(3):380–397

Wiesner C (1970) Hydrometeorology. Chapman and Hall, London, **232 pp**

World Meteorological Organization (1986) Manual for estimation of probable maximum precipitation. Operational Hydrology Report 1, 2nd edition, Publication 332, 269 pp

Yue S, Pilon P, Cavadias G (2002) Power of the Mann-Kendall and Spearman's rho tests for detecting monotonic trends in hydrological series. J Hydrol 259:254–271

AUTHOR QUERIES

AUTHOR PLEASE ANSWER ALL QUERIES.

Q1. Please check the suggested running page title if appropriate. Otherwise, please provide a short running title with a maximum of 65 characters including spaces.
Q2. Please check if the affiliations are correctly presented.
Q3. Please check if the modification is appropriate in the sentence "Intensity–duration–frequency (IDF) curves and their master equation...."
Q4. In Figs. 1, 6, and 7, colored figures were used.
Q5. Please check if all the equations and variables are correctly presented.
Q6. SLP was defined as "sea level pressure." Please check if the definition is correct.
Q7. Please check if the modifications are appropriate in the sentence "The equation corresponds to the enveloping curve...."
Q8. (8) was changed to Eq. (8). Please check if appropriate.
Q9. Please check if the modifications are appropriate in the sentence "The first group contains high-intensity storms...."